



# KR-39038, a Novel GRK5 Inhibitor, Attenuates Cardiac Hypertrophy and Improves Cardiac Function in Heart Failure

Jeong Hyun Lee<sup>1</sup>, Ho Won Seo<sup>1</sup>, Jae Yong Ryu<sup>1</sup>, Chae Jo Lim<sup>1,2</sup>, Kyu Yang Yi<sup>1,2</sup>, Kwang-Seok Oh<sup>1,2,\*</sup> and Byung Ho Lee<sup>1,3,\*</sup>

<sup>1</sup>Therapeutics & Biotechnology Division, Korea Research Institute of Chemical Technology, Daejeon 34114,

<sup>2</sup>Department of Medicinal and Pharmaceutical Chemistry, University of Science and Technology, Daejeon 34113,

<sup>3</sup>Graduate School of New Drug Discovery and Development, Chungnam National University, Daejeon 34134, Republic of Korea

## Abstract

G protein-coupled receptor kinase 5 (GRK5) has been considered as a potential target for the treatment of heart failure as it has been reported to be an important regulator of pathological cardiac hypertrophy. To discover novel scaffolds that selectively inhibit GRK5, we have identified a novel small molecule inhibitor of GRK5, KR-39038 [7-((3-((4-((3-aminopropyl)amino)butyl)amino)propyl)amino)-2-(2-chlorophenyl)-6-fluoroquinazolin-4(3H)-one)]. KR-39038 exhibited potent inhibitory activity (IC<sub>50</sub> value=0.02 μM) against GRK5 and significantly inhibited angiotensin II-induced cellular hypertrophy and HDAC5 phosphorylation in neonatal cardiomyocytes. In the pressure overload-induced cardiac hypertrophy mouse model, the daily oral administration of KR-39038 (30 mg/kg) for 14 days showed a 43% reduction in the left ventricular weight. Besides, KR-39038 treatment (10 and 30 mg/kg/day, p.o.) showed significant preservation of cardiac function and attenuation of myocardial remodeling in a rat model of chronic heart failure following coronary artery ligation. These results suggest that potent GRK5 inhibitor could effectively attenuate both cardiac hypertrophy and dysfunction in experimental heart failure, and KR-39038 may be useful as an effective GRK5 inhibitor for pharmaceutical applications.

**Key Words:** GRK5 inhibitor, KR-39038, Hypertrophy, Heart failure

## INTRODUCTION

G protein-coupled receptor kinase 5 (GRK5) is a multifunctional enzyme capable of shuttling between the cytoplasm and nucleus; it can regulate receptors on the plasma membrane or gene expression in the nucleus in response to various stimuli (Gold *et al.*, 2013; Traynham *et al.*, 2016; Bologna *et al.*, 2017). In particular, GRK5 is highly expressed in the heart and is considered an important regulator of cardiovascular disease pathology (Ping *et al.*, 1997; Lieu and Koch, 2019; Pflieger *et al.*, 2019). GRK5 levels were found to be significantly increased in patients with cardiovascular diseases such as dilated cardiomyopathy and volume overload disorders (Dzimiri *et al.*, 2004; Agüero *et al.*, 2012). Transgenic mice with cardiac-specific overexpression of GRK5 showed increased susceptibility to pressure overload-induced cardiac hypertrophy and cardiac dysfunction, whereas GRK5 knockout mice presented with

attenuated hypertrophic responses (Gold *et al.*, 2012; Hullmann *et al.*, 2014; Traynham *et al.*, 2015). In a myocardial infarction (MI)-induced heart failure model, cardiac-specific GRK5 transgenic mice also showed decreased cardiac function and increased adverse cardiac remodeling compared to non-transgenic littermate control mice (de Lucia *et al.*, 2018). Recent studies demonstrated the possible role of GRK5 in the development of pathological cardiac remodeling. Hypertrophic stimuli induces GRK5 nuclear translocation and subsequently GRK5 increases the expression of hypertrophic genes via regulation of histone deacetylase 5 (HDAC5) (Martini *et al.*, 2008; Gold *et al.*, 2012; Park *et al.*, 2016; Laudette *et al.*, 2019), NF-κB (Islam *et al.*, 2013) and nuclear factor of activated T cell (NFAT) activity (Hullmann *et al.*, 2014; Sorriento *et al.*, 2018). Based on these findings, GRK5 has been recognized as a potential therapeutic target for heart failure due to its pro-hypertrophic effect under pathological conditions. Despite high

**Open Access** <https://doi.org/10.4062/biomolther.2020.129>

This is an Open Access article distributed under the terms of the Creative Commons Attribution Non-Commercial License (<http://creativecommons.org/licenses/by-nc/4.0/>) which permits unrestricted non-commercial use, distribution, and reproduction in any medium, provided the original work is properly cited.

Received Jul 17, 2020 Revised Jul 30, 2020 Accepted Aug 5, 2020

Published Online Sep 1, 2020

### \*Corresponding Authors

E-mail: bhlee@kriict.re.kr (Lee BH), ksoh@kriict.re.kr (Oh KS)

Tel: +82-42-860-7415 (Lee BH), +82-42-860-7547 (Oh KS)

Fax: +82-42-861-4246 (Lee BH), +82-42-861-4246 (Oh KS)

therapeutic potential, little has been reported regarding GRK5 inhibitors under clinical development. In a previous study, amlexanox was identified as a relatively selective GRK5 inhibitor (Homan *et al.*, 2014), but there is still an urgent need for a more potent and selective GRK5 inhibitor.

In our efforts to discover novel small molecules to inhibit GRK5, we identified 7-((3-((4-((3-aminopropyl)amino)butyl)amino)propyl)amino)-2-(2-chlorophenyl)-6-fluoroquinazolin-4(3H)-one (KR-39038, Fig. 1A) as a novel and potent GRK5 inhibitor. The present study aimed to elucidate the pharmacological characteristics of KR-39038 by (i) investigating the effects on GRK5 inhibitory activity and angiotensin II-mediated cellular hypertrophy, (ii) measuring the anti-hypertrophic effect in a mouse model of pressure overload-induced cardiac hypertrophy and (iii) exploring the beneficial effects on cardiac function and fibrosis in a rat model of chronic heart failure following coronary artery ligation.

## MATERIALS AND METHODS

### Materials

Human recombinant GRK5 was purchased from Invitrogen (Carlsbad, CA, USA). The ULight-Histon H3 (Thr3) peptide (5ULight-ARTKQTRKSTG-COOH) and LANCE® time-resolved fluorescence resonance energy transfer (TR-FRET) assay kit was obtained from PerkinElmer (Waltham, MA, USA). KR-39038, 7-((3-((4-((3-aminopropyl)amino)butyl)amino)propyl)amino)-2-(2-chlorophenyl)-6-fluoroquinazolin-4(3H)-one, was synthesized in-house. Dulbecco's modified Eagle's medium, fetal bovine serum, and antibiotics were obtained from GIBCO BRL (Grand Island, NY, USA). All other reagents such as dimethyl sulfoxide, 1 M Tris-HCl (pH 7.4), 1 M MgCl<sub>2</sub>, and reference compounds such as amlexanox and staurosporine were purchased from Sigma-Aldrich (St. Louis, MO, USA).

### In vitro TR-FRET assay for GRK5 activity

Inhibition of kinase activity against GRK5 was measured using LANCE® TR-FRET (PerkinElmer). The ATP concentra-

tion (20  $\mu$ M) was adjusted to equal  $K_m$  and the concentration of GRK5 (0.5  $\mu$ g/mL) and ULight-Histon H3 substrate (80 nM) were used at an EC<sub>50</sub> value. The total reaction volume was 10  $\mu$ L and test compounds were preincubated with enzyme for 10 min before adding the peptide substrate and ATP. Kinase reactions were conducted for 1 h at room temperature in standard 384-well plates and then 10  $\mu$ L of detection mixture including 10 mM EDTA and 1  $\mu$ M europium-tagged antibody supplied by PerkinElmer was added to reaction plates 1 h before reading the plates. Following the addition of reagents for detection, the TR-FRET signal was measured using an EnVision multi-label reader (PerkinElmer). The instrument settings were adjusted to 340 nm for excitation, and 615 nm and 665 nm for emission with a 100  $\mu$ s delay time. IC<sub>50</sub> values were calculated by non-linear regression using Prism version 5.01 (GraphPad Software Inc., La Jolla, CA, USA).

### Animals

Male C57BL/6 mice and Sprague-Dawley (S.D.) rats were purchased from Orient Bio Inc (Sungnam, Korea). Animals were housed in an environmentally controlled room (temperature: 22.0  $\pm$  2°C, humidity: 55  $\pm$  5%, a cycle of 12 h light/dark), and received water and food ad libitum. All experimental procedures described in this study were approved by the Institutional Animal Care and Use Committee of the Korea Research Institute of Chemical Technology in Daejeon, Korea.

### Isolation and cellular hypertrophy of neonatal cardiomyocytes

Primary neonatal cardiomyocytes were isolated from S.D. rats (1-2 days old) using primary myocardial cell isolation kit (Thermo Fisher Scientific Inc., Waltham, MA, USA). The culture medium consisted of DMEM supplemented with 10% FBS, 1% penicillin/streptomycin, and myocardial cell growth supplement. Neonatal cardiomyocytes were maintained at a density of 3  $\times$  10<sup>5</sup> cells per 60-mm dish and then subjected to cellular hypertrophy. After pretreatment with KR-39038 in serum-free media for 24 h, the cells were treated with 0.1  $\mu$ M angiotensin II in quiescence medium (DMEM with 0.5% FBS)

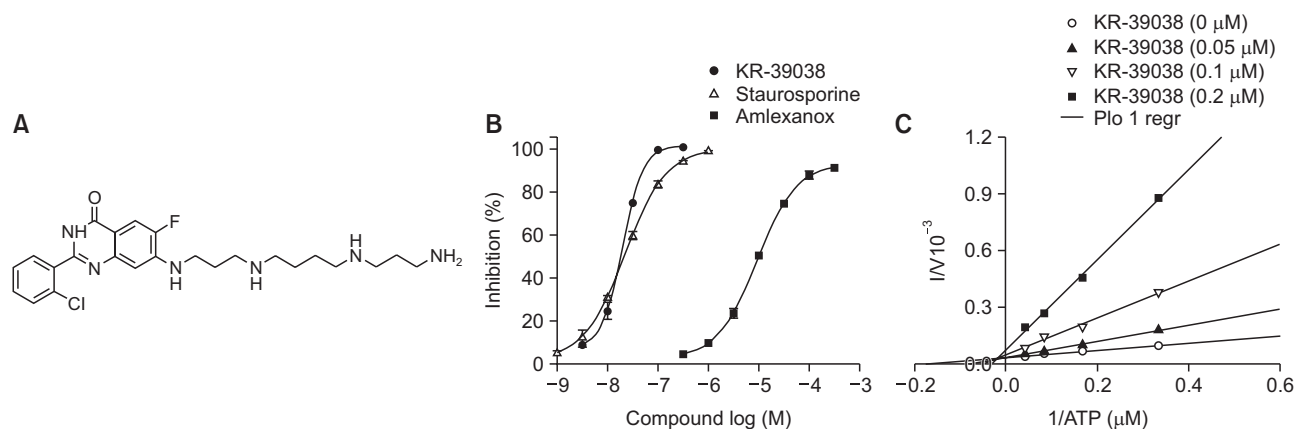


**Fig. 1.** Inhibitory effects of KR-39038 on G protein-coupled receptor kinase 5 (GRK5) activity. (A) Chemical structure of KR-39038. (B) Concentration-response curves of KR-39038, staurosporine and amlexanox for time-resolved fluorescence resonance energy transfer (TR-FRET) based GRK5 kinase assay. (C) Inhibitory mode of KR-39038 in double reciprocal plots of  $1/v$  versus  $1/[ATP]$ . The initial rate  $v$  was estimated as the amount of phospho-substrate transferred during the reaction period (nM/min). Each data point was represented from experiments in triplicate or more.

with or without a fresh supply of KR-39038 for another 4 days to induce a hypertrophic response. After the hypertrophic reaction, cells were fixed with 1% glutaraldehyde (Sigma-Aldrich) and stained with 0.1% crystal violet (Sigma-Aldrich) for 1 h. Cell images were captured with a digital camera mounted on the inverted microscope (Nikon, Tokyo, Japan) and analyzed with the Image-Pro PLUS software (Media Cybernetics, Silver Spring, MD, USA). The average cell surface area was determined by counting over 140 individual cells per well.

### Western blot analysis

Loading samples (30  $\mu$ g) were separated on 10 % sodium dodecyl sulfate-polyacrylamide gel and transferred to nitrocellulose membranes (Hybond-C Extra; GE Healthcare, Piscataway, NJ, USA). After blocking with 5% (w/v) skim milk for 1 h, the membrane was incubated overnight with primary antibody (1:1000; Cell Signaling Technology, Beverly, MA, USA) against the total or phosphorylated form of HDAC5, followed by incubation with secondary antibody (horseradish peroxidase-conjugated anti-mouse at dilutions of 1:1000; Cell Signaling Technology). Protein bands were detected using the SuperSignal West Femto kit (Thermo Fisher Scientific Inc.). The value for phosphorylated HDAC5 was normalized to total HDAC5 expression.

### Transverse aortic constriction in mice

Male C57BL/6 mice (20-24 g) were anesthetized by intraperitoneal injection of Zoletil (30 mg/kg) and Rompun (10 mg/kg). The mice were intubated and ventilated with room air using a small animal ventilator (SAR-830/P; CWE, Inc., Ardmore, PA, USA) and body temperature was maintained at 37°C with a temperature-controlled heating pad. After a midline sternotomy, the transverse aortic arch between the innominate artery and the left common carotid artery was ligated with a blunt 26-gauge needle using 6-0 silk sutures, and the needle was quickly removed. Sham-operated mice were subjected to the same surgical procedure without constricting the aorta. KR-39038 (30 mg/kg), captopril (30 mg/kg; Sigma-Aldrich) or vehicle (0.5% carboxymethyl cellulose) were administered orally once a day for 2 weeks starting from 24 h after the operation. Captopril, an angiotensin-converting enzyme inhibitor, was used to compare the *in vivo* effects of KR-39038. Two weeks after transverse aortic constriction (TAC), the hearts were dissected and weighed and tibia length was measured using a caliper. Cardiac hypertrophy was assessed by determining the ratio of tibia length to heart weight or left ventricular weight.

### Coronary artery ligation in rats

Myocardial infarction (MI) was induced by permanent ligation of the left anterior descending coronary artery. Briefly, after left thoracotomy of male S.D. rats (380-420 g), the coronary artery was ligated using 6-0 silk sutures under isoflurane anesthesia (5% induction, 2-3% maintenance in 100% O<sub>2</sub>) and maintained at 60 beats/min, with a tidal volume of 1.5-2 mL/100g body weight by mechanical ventilation with room air using a small animal ventilator (Harvard Apparatus, Holliston, MA, USA). The rats were randomly assigned to five experimental groups as follows: sham-operated group (n=7), MI+vehicle group (n=11), MI+10 mg/kg/day KR-39038 group (n=10), MI+30 mg/kg/day KR-39038 group (n=9) and MI+30 mg/kg/day captopril group (n=9). All treatments were administered orally once a day for 12 weeks starting from 24 h after

surgery. To adjust the dose accordingly, body weights were measured once a week.

### Echocardiography

The rats were anesthetized with 1.5-3% isoflurane and placed in the supine position on an imaging stage. After shaving the anterior chest and applying gel, transthoracic echocardiography was performed with high-resolution ultrasound (20 MHz) imaging system (Vevo2100, VisualSonics, Ontario, Canada). The LV fractional shortening (FS) and ejection fraction (EF) were measured before surgery (baseline) and after 1, 2, 4, 8, and 12 weeks of left anterior descending coronary artery ligation. The echocardiographic images were analyzed using VisualSonic analysis software by a blinded investigator.

### Histologic analysis

Twelve weeks after ligation of the left anterior descending coronary artery, the heart was incised, weighed, fixed with 10% neutral buffered formalin, and embedded in paraffin. Tissue sections (4  $\mu$ m) were stained with hematoxylin and eosin solution (ScyTek Laboratories, Logan, UT, USA) to measure cardiomyocyte area and Masson's trichrome stain kit (Diagnostic BioSystems, Pleasanton, CA, USA) to examine cardiac fibrosis. The average of cardiomyocyte cross-sectional area was measured using an image analyzing system Image-Pro PLUS software (Media Cybernetics). Collagen deposition in the infarct border zone was expressed as percentage of the fibrous tissue area in the entire visual field.

### Pharmacokinetic study

The plasma concentration of KR-39038 was measured in S.D. rats (260-300 g) following single intravenous (5 mg/kg) or oral (300 mg/kg) administration. Plasma was collected at 0.08, 0.25, 0.5, 0.75, 1, 2, 4, 6, 8 and 24 h after dosing, and the plasma levels of KR-39038 were measured using high-performance liquid chromatography with tandem mass spectrometry (LC-MS/MS). To assess tissue distribution, KR-39038 was injected intravenously at a dose of 10 mg/kg. Tissue samples (heart, brain, liver, lung, and kidney) and plasma samples were collected at 10 min or 4 h after the administration of KR-39038.

### Statistical analysis

The values from biochemical and cell-based assays were expressed as mean  $\pm$  SD, while values for animal-based studies were expressed as mean  $\pm$  SEM. Concentration-response curves were analyzed using PRISM version 5.0 (GraphPad Software Inc.). Data were analyzed by one-way analysis of variance followed by Dunnett's test for multiple comparisons (Sigma Stat, Jandel Co., San Rafael, CA, USA). Statistical significance was observed for *p* values less than 0.05 for all comparisons.

## RESULTS

### Inhibitory effects on GRK5 activity

The inhibitory effect of KR-39038 on the activity of GRK5 was evaluated using a TR-FRET-based GRK5 kinase assay. The assay conditions of GRK5 kinase were verified with staurosporine and amlexanox as reference compounds (IC<sub>50</sub> values: 0.02  $\pm$  0.003 and 8.86  $\pm$  0.72  $\mu$ M, respectively). As

shown in Fig. 1B, KR-39038 inhibited GRK5-induced TR-FRET counts in a concentration-dependent manner, and the  $IC_{50}$  value was  $0.02 \pm 0.01 \mu\text{M}$ . In the inhibitory mode studies, double reciprocal plots of  $1/v$  versus  $1/[ATP]$  were obtained at various concentrations of ATP ( $0.625\text{--}10 \mu\text{M}$ ) and GRK5 ( $0.1 \mu\text{g/mL}$ ) with or without increasing concentrations of KR-39038. As shown in Fig. 1C, KR-39038 behaved as a mixed inhibitor of GRK5.

### Inhibitory effects on angiotensin II-induced cellular hypertrophy and phosphorylation of histone deacetylase 5 in neonatal cardiomyocytes

The anti-hypertrophic effects of KR-39038 and amlexanox on neonatal rat cardiomyocytes were determined by incubation with angiotensin II ( $0.1 \mu\text{M}$ ) for 4 days in the presence or absence of KR-39038 or amlexanox. Cells treated with angiotensin II exhibited an increase of  $\sim 58\%$  in cell surface area, and this cellular hypertrophic effect was concentration-dependently inhibited by both KR-39038 and amlexanox. In particular, angiotensin II-induced cellular hypertrophy was significantly inhibited by KR-39038 at a concentration of  $0.1 \mu\text{M}$  and higher concentrations. The efficacy of KR-39038 was approximately 30 times higher than that of amlexanox (Fig.

2A, 2B).

To assess the effects of KR-39038 on the phosphorylation of HDAC5 via GRK5 activation, we prepared extracts of angiotensin II-activated neonatal cardiomyocytes and determined the level of phosphorylated HDAC5 by immunoblotting (Fig. 2C). Treatment with  $0.1 \mu\text{M}$  angiotensin II for 15 min resulted in the induction of HDAC5 phosphorylation in neonatal cardiomyocytes and angiotensin II-induced HDAC5 phosphorylation was decreased by pretreatment with KR-39038 at  $0.3 \mu\text{M}$  and higher concentrations. Amlexanox was used as a reference (Fig. 2C).

### Anti-hypertrophic activity in a pressure-overloaded model in mice

C57BL/6 mice were subjected to transverse aortic constriction (TAC) or sham surgery to evaluate the effect of KR-39038 against pressure overload-induced cardiac hypertrophy. After 24 h of TAC, KR-39038 ( $30 \text{ mg/kg}$ ), captopril ( $30 \text{ mg/kg}$ ) or vehicle were orally administered once a day for 2 weeks. After 2 weeks of TAC (Fig. 3A), the left ventricular weight-to-tibia length ratio ( $6.7 \pm 0.2$  and  $4.7 \pm 0.1 \text{ mg/mm}$ , respectively,  $p < 0.05$ , Fig. 3B) and heart weight-to-tibia length ratio ( $8.2 \pm 0.2$  and  $6.2 \pm 0.1 \text{ mg/mm}$ , respectively,  $p < 0.05$ , Fig. 3C) were

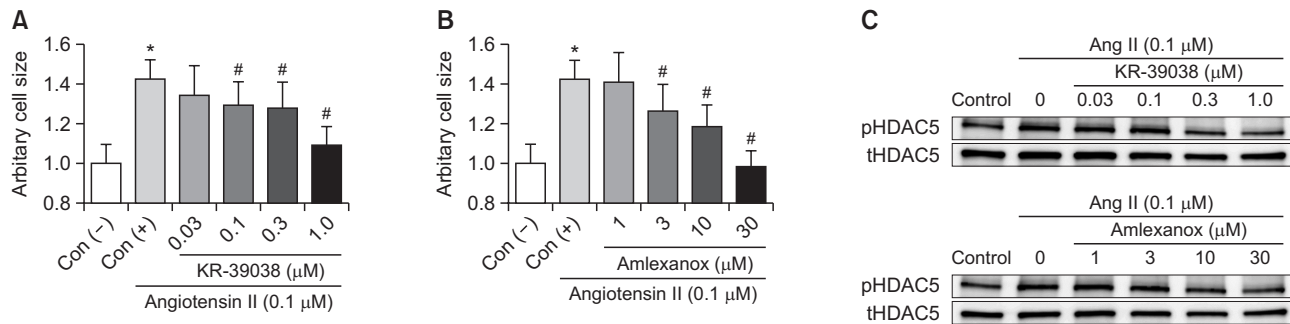


**Fig. 2.** Anti-hypertrophic effects of (A) KR-39038 and (B) amlexanox in neonatal cardiomyocytes. (C) Inhibition of KR-39038 and amlexanox against angiotensin II (Ang II)-induced phosphorylation of histone deacetylase 5 (HDAC5). After inducing cellular hypertrophy with  $0.1 \mu\text{M}$  angiotensin II, adherent cells were fixed and stained to obtain images for analysis. Targeted cell size was analyzed using Image-Pro PLUS software (Media Cybernetics, Silver Spring, MD, USA), and the relative cell sizes were expressed as mean  $\pm$  SD ( $n=15$ ). \* $p < 0.05$ , significantly different from negative control (Con (-)), # $p < 0.05$ , significantly different from positive control (Con (+)) stimulated with  $0.1 \mu\text{M}$  angiotensin II.

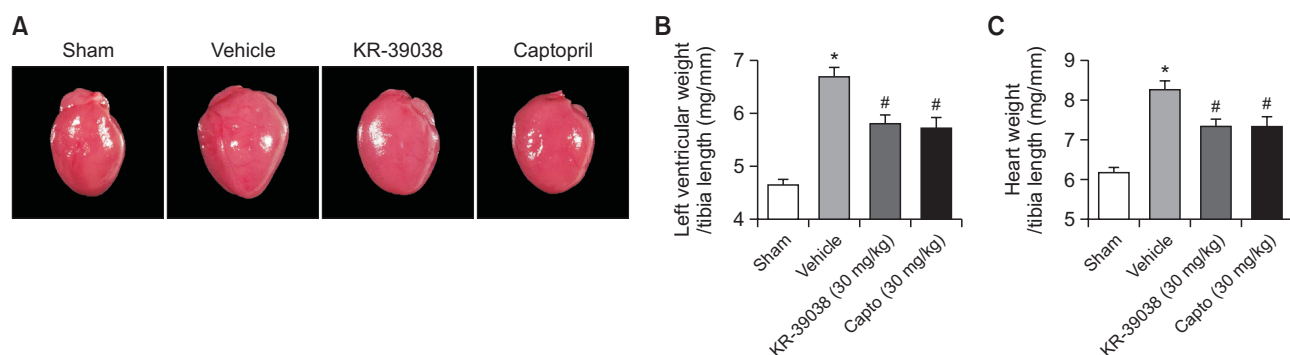


**Fig. 3.** Effects of KR-39038 on cardiac hypertrophy in transverse aortic constriction (TAC) model in mice. (A) Representative gross hearts. (B) Left ventricular weight-to-tibia length ratio and (C) heart weight-to-tibia length ratio were measured at 2 weeks after transverse aortic constriction (TAC). Values are mean percentage  $\pm$  SEM ( $n=15\text{--}17$ ). \* $p < 0.05$ , significantly different from the sham-operated group and # $p < 0.05$ , significantly different from the vehicle-treated group. Capto, Captopril.



remarkably increased in the vehicle-treated group compared to the sham group. However, the treatment with KR-39038 (30 mg/kg) significantly attenuated the development of cardiac hypertrophy compared with the vehicle-treated group ( $5.8 \pm 0.2$  and  $7.3 \pm 0.2$  mg/mm for left ventricular weight-to-tibia length ratio and heart weight-to-tibia length ratio, respectively,

$p < 0.05$ ). This anti-hypertrophic effect by KR-39038 was similar to that of captopril (Fig. 3).

**Cardioprotective effects in a post-MI heart failure model in rats.**

The anti-hypertrophic and cardioprotective effects of KR-

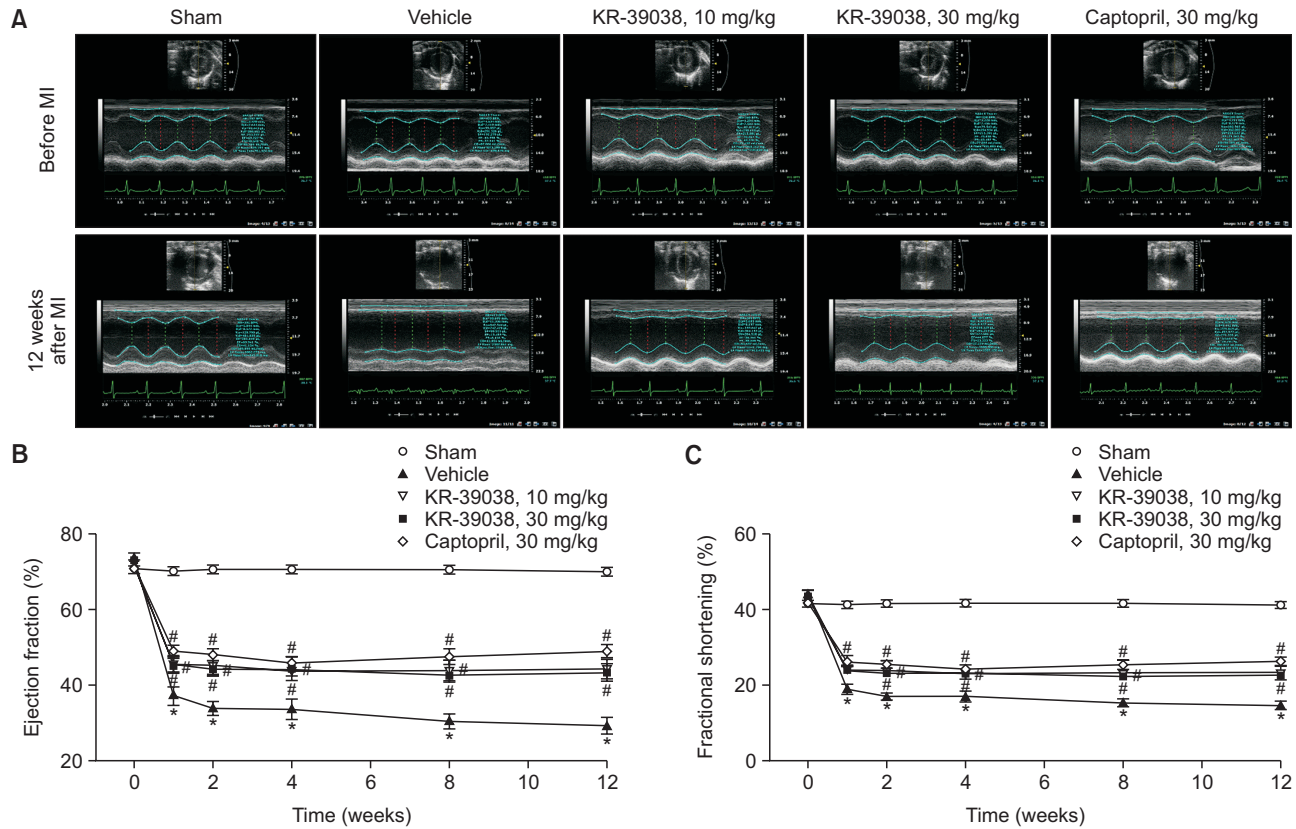


**Fig. 4.** Echocardiographic measurements. (A) Representative M-mode echocardiographic images, (B) left ventricular ejection fraction and (C) Fractional shortening from sham-operated group, myocardial infarction (MI)+vehicle, MI+KR-39038 (10 mg/kg), MI+KR-39038 (30 mg/kg), and MI+captopril groups at 12 weeks after coronary artery ligation. Values are mean percentage  $\pm$  SEM ( $n=7-12$ ). \* $p < 0.05$ , significantly different from the sham-operated group and # $p < 0.05$ , significantly different from the vehicle-treated group.

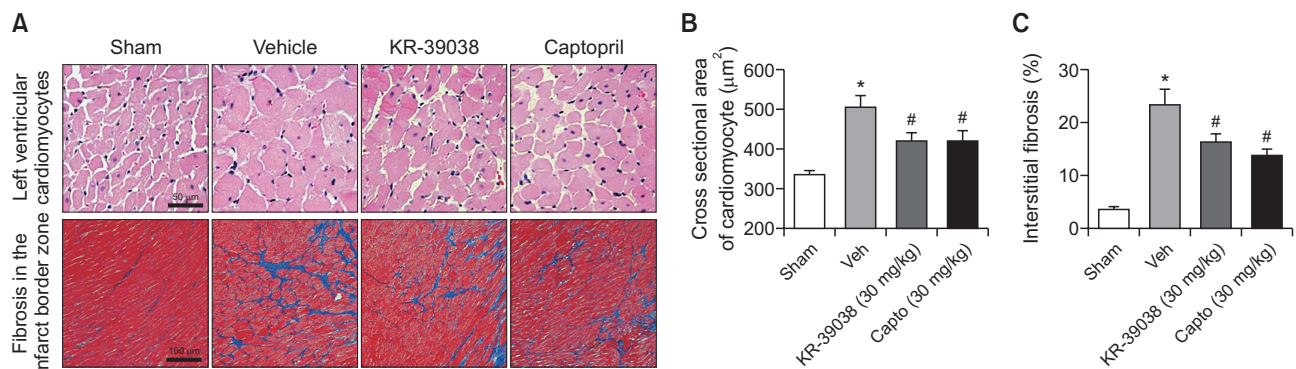


**Fig. 5.** Effects of KR-39038 on cardiac hypertrophy and fibrosis in myocardial infarction (MI)-induced heart failure in rats. (A) Representative photomicrographs of sections stained with hematoxylin & eosin and Masson's trichrome in the peri-infarct zone of each group. (B) The cross-sectional area of cardiomyocytes ( $\mu\text{m}^2$ ), and (C) interstitial fibrosis (%) were determined 12 weeks after coronary artery ligation. Values are mean percentage  $\pm$  SEM ( $n=7-8$ ). \* $p < 0.05$ , significantly different from the sham-operated group and # $p < 0.05$ , significantly different from the vehicle (Veh)-treated group. Capto, Captopril.

39038 were confirmed in another animal model of cardiac remodeling following the induction of chronic MI in rats. The survival rates were 53%, 67%, 80% and 73% in the vehicle-, captopril-, 10 and 30 mg/kg KR-39038-treated groups, respectively. The effect of KR-39038 on cardiac function was examined by echocardiography in myocardial infarction model in rats at 1, 2, 4, 8, and 12 weeks after coronary artery ligation. Representative echocardiographic images are shown in Fig. 4A. As shown in Fig. 4B, 4C, the ligation of coronary artery caused a gradual decrease in ejection fraction and fractional shortening in the vehicle-treated group. However, the groups treated with KR-39038 ameliorated cardiac dysfunction over time. At 12 weeks after coronary artery ligation, the vehicle-treated group was found to have significantly lower left ventricular ejection fraction ( $29.2 \pm 2.1\%$  and  $69.9 \pm 1.0\%$ , respectively,  $p < 0.05$ ) and fractional shortening ( $14.6 \pm 1.1\%$  and  $41.1 \pm 0.9\%$ , respectively,  $p < 0.05$ ) than that of the sham group. The 10 and 30 mg/kg KR-39038-treated groups exhibited a prominent elevation of left ventricular ejection fraction ( $44.3 \pm 2.6\%$  and  $43.4 \pm 2.3\%$ , respectively) compared to the vehicle-treated groups ( $p < 0.05$ ), and showed a significant increase in fractional shortening ( $23.4 \pm 1.6\%$  and  $22.6 \pm 1.3\%$ , respectively).

After echocardiographic assessment, we performed hematoxylin and eosin and Masson's trichrome staining with the left ventricles to measure the cross-sectional area of cardiomyocytes and interstitial fibrosis, respectively (Fig. 5A). There were no significant difference in the ratio of a left ventricular

weight to body weight among the groups, but the myocyte cross-sectional area ( $504.6 \pm 29.5 \mu\text{m}^2$  and  $336.7 \pm 9.9 \mu\text{m}^2$ , respectively) and interstitial fibrosis ( $23.3 \pm 2.9\%$  and  $3.7 \pm 0.5\%$ , respectively) were significantly increased in the vehicle-treated group compared with the sham group at 12 weeks after MI (Fig. 5B, 5C). MI-induced enlargement of cardiomyocytes and interstitial fibrosis were significantly decreased by the administration of 30 mg/kg KR-39038 ( $420.1 \pm 21.2 \mu\text{m}^2$  and  $16.3 \pm 1.6\%$ , respectively). The cardioprotective effects of KR-39038 were comparable to those of the captopril group (Fig. 4, 5).

### Pharmacokinetic study

The primary PK parameters for KR-39038 are summarized in Table 1. The  $\text{AUC}_{0-\infty}$  values after intravenous injection with 10 mg/kg and oral administration of 300 mg/kg of KR-39038 were  $3.4 \pm 1.0$  and  $8.9 \pm 5.0 \mu\text{g}\cdot\text{h/mL}$ , respectively, resulting in 4.3% bioavailability. The  $t_{1/2}$  values after intravenous injection and oral administration were  $0.7 \pm 0.04$  and  $2.3 \pm 2.9$  h, respectively. Interestingly, 4 h after intravenous injection of KR-39038, its concentration in cardiac tissue was 16.9 times higher than that in plasma (Table 2). Furthermore, the concentrations of KR-39038 in the brain, liver, lung and kidney were 11.3, 10.4, 2.7 and 26.3 times higher than that in plasma, respectively.

### DISCUSSION

In the present study, we investigated the pharmacological properties of KR-39038, a novel GRK5 inhibitor, through biochemical and cellular assays, and animal models of cardiac hypertrophy and heart failure. In our efforts to discover novel small molecules that inhibit GRK5, we have developed a new and potent GRK5 inhibitor, 7-((3-((4-((3-aminopropyl)amino)butyl)amino)propyl)amino)-2-(2-chlorophenyl)-6-fluoroquinazolin-4(3H)-one (KR-39038). KR-39038 was generated from members of 2-aryl substituted quinazoline-4(3H)-one derivatives based on the results of extensive and systematic structure-activity relationship (SAR) investigation of quinazoline-4(3H)-one with 2-aryl groups possessing a variety of substituents. In addition, the spermine group of KR-39038 at 7-position appears to play a significant role in the strong inhibition of GRK5. KR-39038 showed greater inhibitory effect ( $\text{IC}_{50}$  value:  $0.02 \mu\text{M}$ ) on GRK5 than that of the known GRK5 inhibitor, amlexanox ( $\text{IC}_{50}$  value:  $8.86 \mu\text{M}$ ). Furthermore, the inhibitory activity of KR-39038 against GRK2 showed 5.9% inhibition at  $10 \mu\text{M}$ . In addition, the inhibitory mode of KR-39038

**Table 1.** Pharmacokinetic parameters of KR-39038

Parameters	5 mg/kg (i.v.)	300 mg/kg (p.o.)
$C_{max}$ ( $\mu\text{g/mL}$ )	NA	$5.2 \pm 2.8$
$T_{max}$ (h)	NA	$0.7 \pm 0.2$
$t_{1/2}$ (h)	$0.7 \pm 0.04$	$2.3 \pm 2.9$
$\text{AUC}_{0-\infty}$ ( $\mu\text{g}\cdot\text{h/mL}$ )	$3.4 \pm 1.0$	$8.9 \pm 5.0$
CL (L/h/kg)	$1.6 \pm 0.5$	NA
Vss (L/kg)	$1.2 \pm 0.2$	NA
F (%)		$4.3 \pm 2.4$

The pharmacokinetic parameters were determined as described in Method 2.10.  $C_{max}$ , maximum concentration;  $T_{max}$ , time at maximum;  $t_{1/2}$ , terminal half-life;  $\text{AUC}_{0-\infty}$ , area under the concentration curve; CL, clearance; Vss, volume of distribution at steady state; F (%), oral bioavailability; NA, not applicable. The values are expressed as mean  $\pm$  SEM of three animals.

**Table 2.** Concentration of KR-39038 in plasma, heart, brain, liver, lung and kidney tissues in rats

Tissue	Concentration (ng/mL or ng/g tissue)		Kp (ratio of tissue to plasma concentration)	
	10 min	4 h	10 min	4 h
Plasma	$6323.3 \pm 326.2$	$246.7 \pm 35.2$	1	1
Heart	$986.7 \pm 215.9$	$4162.7 \pm 148.7$	0.2	16.9
Brain	$981.3 \pm 142.0$	$2798.7 \pm 1279.5$	0.2	11.3
Liver	$1096.0 \pm 179.2$	$2576.0 \pm 943.5$	0.2	10.4
Lung	$248.4 \pm 63.1$	$676.0 \pm 181.7$	0.04	2.7
Kidney	$9666.7 \pm 1335.3$	$6480.0 \pm 1076.3$	1.5	26.3

The values are expressed as mean  $\pm$  SEM of 3 animals.

served as a mixed inhibitor of GRK5. Although the concepts of a mixed inhibitor, KR-39038 may be more selective than other ATP-competitive inhibitors. Selective GRK5 inhibitors are desirable because they can reduce off-target effects and provide more flexibility in combination therapy.

Cardiac hypertrophy is an important risk factor for heart failure and other cardiovascular diseases (Dickhout *et al.*, 2011). Interestingly, it has been found that the non-canonical function of GRK5, which regulates the transcription of genes, plays a key role in maladaptive cardiac hypertrophy and heart failure (Belmonte and Blaxall, 2012; Hullmann *et al.*, 2016; Lieu and Koch, 2019). Several studies have demonstrated that GRK5 regulates cardiomyocyte hypertrophy in response to a subset of hypertrophic stimuli such as angiotensin II, phenylephrine and urotensin II, mainly through its ability to phosphorylate HDAC5, leading to nuclear HDAC5 export and subsequently inducing gene expression involved in cardiomyocyte hypertrophy (Zhang *et al.*, 2011; Park *et al.*, 2016; Oda *et al.*, 2018).

Our cell-based studies showed that GRK5 inhibitors, KR-39038 and amlexanox, significantly inhibited angiotensin II-induced cellular hypertrophy in neonatal cardiomyocytes. In addition, exposure to angiotensin II (0.1  $\mu$ M) resulted in an increase in HDAC5 phosphorylation in neonatal cardiomyocytes. However, angiotensin II-induced phosphorylation of HDAC5 was effectively downregulated by KR-39038 and amlexanox. Therefore, our results are in agreement with findings from previous studies, suggesting that KR-39038 ameliorates angiotensin II-induced cardiomyocyte hypertrophy, at least in part, through inhibition of GRK5-mediated HDAC5 phosphorylation and subsequent hypertrophic gene expression.

GRK5 levels were found to be significantly increased in patients with cardiovascular diseases (Dzimiri *et al.*, 2004; Agüero *et al.*, 2012). The detrimental effects of GRK5 have been described in transgenic mice with cardiac-specific overexpression of GRK5 following pressure overload and ischemic heart failure (Hullmann *et al.*, 2014; de Lucia *et al.*, 2018). In addition, GRK5 knockout mice are less susceptible to chronic phenylephrine infusion and pressure overload-induced cardiac hypertrophy and cardiac dysfunction (Gold *et al.*, 2012; Hullmann *et al.*, 2014). These findings strongly suggest that GRK5 could be a potential therapeutic target to limit maladaptive cardiac remodeling. However, the effects of selective GRK5 inhibitors has not been evaluated in cardiovascular disease models because few small molecule inhibitors have been identified that potently inhibit the GRK5. In the present study, we examined the effects of KR-39038 on animal models of cardiac hypertrophy and ischemic heart failure to assess its *in vivo* efficacy. Consistent with the *in vitro* results of cellular hypertrophy, oral administration of KR-39038 (30 mg/kg) significantly decreased the development of pressure overload-induced left ventricular hypertrophy in mice. Along with the anti-hypertrophic effect in TAC mice, oral administration of KR-39038 (10 and 30 mg/kg) for 12 weeks after coronary artery ligation in rats significantly improved cardiac function and reduced adverse ventricular remodeling by attenuating interstitial collagen deposition and cardiomyocyte enlargement compared with those in the vehicle-treated group (Fig. 4, 5).

Pharmacokinetic studies have shown that KR-39038 has low bioavailability as low as 4%. However, 4 h after intravenous injection of KR-39038, the concentration of KR-39038 in cardiac tissue was 16.9 times higher than that in plasma. Moreover, the concentration of KR-39038 in cardiac tissue

(4.2  $\mu$ g/mL) was 440 times higher than the IC<sub>50</sub> value of KR-39038 for GRK5 inhibition (0.02  $\mu$ M). These results suggest that KR-39038 exerts direct inhibitory effects on adverse cardiac remodeling and dysfunction. In a preliminary studies, KR-39038 showed low cytotoxicity (EC<sub>50</sub> values: 61.1, 89.9, >100, >100 and >100  $\mu$ M for NIH3T3, L929, VERO, HFL-1 and CHO-K1 cell lines, respectively) and cardiotoxicity (IC<sub>50</sub> value of patch clamp for the hERG channel: >50  $\mu$ M). In addition, in acute toxicity studies with male S.D. rats, LD<sub>50</sub> value exceeded 1000 mg/kg by oral administration.

Few studies have reported positive effects of GRK5 inhibitors in an animal disease model of ventricular hypertrophy. Here, we report for the first time a novel GRK5 inhibitor possessing potent anti-hypertrophic effects both in pressure-overloaded and infarcted rodent hearts. Our findings demonstrate that KR-39038 is a novel GRK5 inhibitor with high inhibitory activity. Angiotensin II-induced cellular hypertrophy in neonatal cardiomyocytes was significantly inhibited by KR-39038 through suppression of HDAC5 pathway. In particular, oral administration of KR-39038 significantly prevented cardiac hypertrophy after pressure overload in mice and showed profound anti-hypertrophic effects and improved cardiac function following left anterior descending artery ligation in rats. These findings increase the possibility of GRK5 inhibitors as potential treatment options for heart failure. In addition, KR-39038 may be useful as an effective GRK5 inhibitor for pharmaceutical applications.

## CONFLICT OF INTEREST

The authors declare that there is no conflict of interests.

## ACKNOWLEDGMENTS

This research was supported by Korea Drug Development Fund (KDDF) funded by MSIP, MOTIE and MOHW (KDDF-201603-01, Republic of Korea).

## REFERENCES

- Agüero, J., Almenar, L., Montó, F., Oliver, E., Sánchez-Lázaro, I., Vicente, D., Martínez-Dolz, L., D'Ocon, P., Rueda, J. and Salvador, A. (2012) Myocardial G protein receptor-coupled kinase expression correlates with functional parameters and clinical severity in advanced heart failure. *J. Card. Fail.* **18**, 53-61.
- Belmonte, S. L. and Blaxall, B. C. (2012) G protein-coupled receptor kinase 5: exploring its hype in cardiac hypertrophy. *Circ. Res.* **111**, 957-958.
- Bologna, Z., Teoh, J. P., Bayoumi, A. S., Tang, Y. and Kim, I. M. (2017) Biased G protein-coupled receptor signaling: new player in modulating physiology and pathology. *Biomol. Ther. (Seoul)* **25**, 12-25.
- de Lucia, C., Grisanti, L. A., Ibbett, J., Lucchese, A. M., Gao, E., Tilley, D. G., Leosco, D., Ferrara, N., Rengo, G. and Koch, W. J. (2017) GRK5-mediated exacerbation of ischemic heart failure involves cardiac immune-inflammatory responses. *Cir. Res.* **121**, A396.
- Dickhout, J. G., Carlisle, R. E. and Austin, R. C. (2011) Interrelationship between cardiac hypertrophy, heart failure, and chronic kidney disease: endoplasmic reticulum stress as a mediator of pathogenesis. *Circ. Res.* **108**, 629-642.
- Dzimiri, N., Muiya, P., Andres, E. and Al-Halees, Z. (2004) Differential functional expression of human myocardial G protein receptor kinases in left ventricular cardiac diseases. *Eur. J. Pharmacol.* **489**,

- 167-177.
- Gold, J. I., Gao, E., Shang, X., Premont, R. T. and Koch, W. J. (2012) Determining the absolute requirement of G protein-coupled receptor kinase 5 for pathological cardiac hypertrophy: short communication. *Circ. Res.* **111**, 1048-1053.
- Gold, J. I., Martini, J. S., Hullmann, J., Gao, E., Chuprun, J. K., Lee, L., Tilley, D. G., Rabinowitz, J. E., Bossuyt, J., Bers, D. M. and Koch, W. J. (2013) Nuclear translocation of cardiac G protein-coupled Receptor kinase 5 downstream of select Gq-activating hypertrophic ligands is a calmodulin-dependent process. *PLoS ONE* **8**, e57324.
- Homan, K. T., Wu, E., Cannavo, A., Koch, W. J. and Tesmer, J. J. (2014) Identification and characterization of amlexanox as a G protein-coupled receptor kinase 5 inhibitor. *Molecules* **19**, 16937-16949.
- Hullmann, J. E., Grisanti, L. A., Makarewich, C. A., Gao, E., Gold, J. I., Chuprun, J. K., Tilley, D. G., Houser, S. R. and Koch, W. J. (2014) GRK5-mediated exacerbation of pathological cardiac hypertrophy involves facilitation of nuclear NFAT activity. *Circ. Res.* **115**, 976-985.
- Hullmann, J., Traynham, C. J., Coleman, R. C. and Koch, W. J. (2016) The expanding GRK interactome: implications in cardiovascular disease and potential for therapeutic development. *Pharmacol. Res.* **110**, 52-64.
- Islam, K. N., Bae, J. W., Gao, E. and Koch, W. J. (2013) Regulation of nuclear factor  $\kappa$ B (NF- $\kappa$ B) in the nucleus of cardiomyocytes by G protein-coupled receptor kinase 5 (GRK5). *J. Biol. Chem.* **288**, 35683-35689.
- Laudette, M., Coluccia, A., Sainte-Marie, Y., Solari, A., Fazal, L., Sicard, P., Silvestri, R., Mialet-Perez, J., Pons, S., Ghaleh, B., Blondeau, J. P. and Lezoualc'h, F. (2019) Identification of a pharmacological inhibitor of Epac1 that protects the heart against acute and chronic models of cardiac stress. *Cardiovasc. Res.* **115**, 1766-1777.
- Lieu, M. and Koch, W. J. (2019) GRK2 and GRK5 as therapeutic targets and their role in maladaptive and pathological cardiac hypertrophy. *Expert Opin. Ther. Targets* **23**, 201-214.
- Martini, J. S., Raake, P., Vinge, L. E., DeGeorge, B. R., Jr., Chuprun, J. K., Harris, D. M., Gao, E., Eckhart, A. D., Pitcher, J. A. and Koch, W. J. (2008) Uncovering G protein-coupled receptor kinase-5 as a histone deacetylase kinase in the nucleus of cardiomyocytes. *Proc. Natl. Acad. Sci. U.S.A.* **105**, 12457-12462.
- Oda, T., Yamamoto, T., Kato, T., Uchinoumi, H., Fukui, G., Hamada, Y., Nanno, T., Ishiguchi, H., Nakamura, Y., Okamoto, Y., Kono, M., Okuda, S., Kobayashi, S., Bers, D. M. and Yano, M. (2018) Nuclear translocation of calmodulin in pathological cardiac hypertrophy originates from ryanodine receptor bound calmodulin. *J. Mol. Cell. Cardiol.* **125**, 87-97.
- Park, C. H., Lee, J. H., Lee, M. Y., Lee, J. H., Lee, B. H. and Oh, K. S. (2016) A novel role of G protein-coupled receptor kinase 5 in uro-tensin II-stimulated cellular hypertrophy in H9c2<sub>UT</sub> cells. *Mol. Cell. Biochem.* **422**, 151-160.
- Pflegger, J., Gresham, K. and Koch, W. J. (2019) G protein-coupled receptor kinases as therapeutic targets in the heart. *Nat. Rev. Cardiol.* **16**, 612-622.
- Ping, P., Anzai, T., Gao, M. and Hammond, H. K. (1997) Adenylyl cyclase and G protein receptor kinase expression during development of heart failure. *Am. J. Physiol.* **273**, H707-H717.
- Sorriento, D., Santulli, G., Ciccarelli, M., Maione, A. S., Illario, M., Trimarco, B. and Iaccarino, G. (2018) The amino-terminal domain of GRK5 inhibits cardiac hypertrophy through the regulation of calcium-calmodulin dependent transcription factors. *Int. J. Mol. Sci.* **19**, 861.
- Traynham, C. J., Cannavo, A., Zhou, Y., Vouga, A. G., Woodall, B. P., Hullmann, J., Ibeti, J., Gold, J. I., Chuprun, J. K., Gao, E. and Koch, W. J. (2015) Differential role of G protein-coupled receptor kinase 5 in physiological versus pathological cardiac hypertrophy. *Circ. Res.* **117**, 1001-1012.
- Traynham, C. J., Hullmann, J. and Koch, W. J. (2016) Canonical and non-canonical actions of GRK5 in the heart. *J. Mol. Cell. Cardiol.* **92**, 196-202.
- Zhang, Y., Matkovich, S. J., Duan, X., Gold, J. I., Koch, W. J. and Dorn, G. W., 2nd (2011) Nuclear effects of G-protein receptor kinase 5 on histone deacetylase 5-regulated gene transcription in heart failure. *Circ. Heart Fail.* **4**, 659-668.